JOURNAL OF ENGINEERING SCIENCES

Volume 7, Issue 2 (2020)

Demianenko, M., Volf, M., Skydanenko M., Yakovchuk V., Pavlenko, I., Liaposhchenko O. (2020). Numerical simulation of the perforated shell's oscillations in a vibrational priller. Journal of Engineering Sciences, Vol. 7(2), pp. F30–F36, doi: 10.21272/jes.2020.7(2).f5

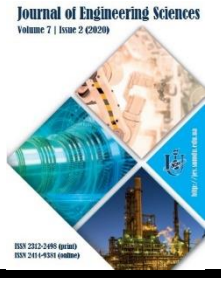

Numerical Simulation of the Perforated Shell's Oscillations in a Vibrational Priller

Demianenko M.[1*][0000-0002-4258-0379], Volf M.[2][0000-0002-2904-8994], Skydanenko M.[1][0000-0002-0277-1867], Yakovchuk V.[1], Pavlenko I.[1][0000-0002-6136-1040], Liaposhchenko O.[1][0000-0002-6657-7051]

[1] Sumy State University, 2, Rymskogo-Korsakova St., 40007 Sumy, Ukraine;
[2] University of West Bohemia, 2738/8, Univerzitni St., 301 00 Pilsen 3, Czech Republic

Article info:
Paper received: October 2, 2020
The final version of the paper received: December 16, 2020
Paper accepted online: December 21, 2020

***Corresponding email:**
m.demianenko@omdm.sumdu.edu.ua

Abstract. The widespread catalysts and nuclear fuel production are the sol-gel technology, including several stages, namely, the raw materials preparation, dispersing it into drops, the granules formation in gas and then in liquid media, granules removal with liquid separation. The vibration granulator is proposed to use on the dispersion stage. One of the problems in their development is determining the vibrational characteristics of a perforated bucket filled with liquid to a certain level. Considering that vibrations are transmitted from the emitter disk through the liquid melt and cause vibrations of the perforated shell, in research, it was decided to use the Fluent Flow and the Transient Structural modules of the ANSYS Workbench software. As a result, numerical simulation results of the emitter disk vibration effect on the cylindrical body are presented. Also, parameters of a discrete mathematical model are evaluated by the bucket vibrations characteristics. The corresponding model considers the inertial, stiffness, and damping properties of functional elements. Additionally, according to the modal analysis results of the priller body, it was determined the eigenfrequencies of the hydromechanical system. Finally, based on the numerical simulation results and their analysis using Fourier transformations, it was determined that the oscillations of the lower part of the bucket, consisting of two harmonic oscillations that equal 230 Hz and 520 Hz.

Keywords: perforated bucket, oscillations, computational fluid dynamics, Fourier transform, parameter identification.

1 Introduction

The creation of new granular materials in an active hydrodynamic environment is carried out using vibrating prillers widely used in various industries.

The reliability and durability of any mechanism is one of the main tasks set for their developers. Vibration plays an essential role in the equipment operating and service life because it may lead to breakdowns. Considering that the main "instrument" for the prillers direct function is vibration, the study of its shell-free vibrations has an essential role for the entire apparatus.

The Fluent Flow and Transient Structural modules of the ANSYS Workbench have been used for the above aim. These calculations are based respectively on the finite volume method and the finite element method. The prillers shell amplitudes and frequencies are determined by the numerical simulation results, which were processed with using the Fast Fourier Transform via the computer algebra system "MathCAD".

The study outcomes will improve the existing vibrating priller design, which will increase efficiency, reliability, and warranty period.

2 Literature Review

The study of the granule's solidification process and the dispersion process using numerical methods is given much attention in the following authors' works.

Numerical modeling of the droplet solidification process in the tower with the subsequent determination of such parameters as the diameter of solidified particles, the temperature profile of the dispersed phase, and the change in the heat transfer coefficient was carried out using CFD methods, namely the Fluent software [1, 2]. Also, in [3, 4], using the computational fluid dynamics methods, the tower height was determined, necessary for the complete specific diameter granules solidification. Article [5] presents research to study the inlet velocity, liquid jet diameter, oscillations amplitude, and frequency influence on the circular laminar fluid jets shape. The minimization

of fines emissions from an industrial drying tower for ammonium nitrate granules production was investigated [6] using CFD methods [7]. The liquid flow in the priller's basket is studied, and the flow rates fields and the outflow rate of melt jets from the holes are determined using CFD methods [8, 9].

Notably, the granulation process study in the above articles using the computational fluid dynamics methods makes it possible to determine the influence of technological regimes and the prillers design on the main process parameters. Also, in many studies, it is indicated that the numerical modeling results of processes occurring in prillers and drying towers give a good similarity with the results of the experiments [10–12].

In conclusion, numerical methods make it possible to determine the vibrational granulation process's main parameters with a sufficient accuracy degree. Based on these results, it seems possible to improve the design and operating regimes of granulation equipment. It should also be noted that the vibrations imposition study on the priller basket and the cylindrical part is not considered in these works.

3 Research Methodology

3.1 The numerical simulation model

The first step of each numerical simulation is computational model development, which includes simplifications for speeding up computations and facilitating the computational grid creation and interpretation results.

For studying the vibration transition from the actuator through the melt to the perforated bottom, at the first stage of calculations, the following simplifications and assumptions are considered:

1) the coupling rod which transmits vibration from the actuator to the emitter disk is rigid, which means that it is possible not to introduce it into the design geometry and set the boundary conditions only for the emitter disk;

2) the water jets that flow out of the perforated bucket does not affect its vibrations. Therefore, at the first stage of calculations, they will not be considered;

3) assumed that the cylindrical body and the perforated bucket are stationary.

The resulting design geometry is shown in Figure 1. The geometry was additionally divided into zones to accuracy calculations ensuring. The finite-volume mesh settings for the Fluent Flow module are the next one. For zone 1, the Sweep method (optimal for Boolean bodies) was used with the following setting: Number of Division – 25; Element Order – Linear; Free Face Meshing Type – Quad. The same method was used for zone 2: Number of Division – 75; Element Order – Linear; Free Face Meshing Type – Quad. The “Multi Zone” method was used for zones 3, 5, and 6 with the “Hex Dominant” setting, which allows building the Hexsa-Elements Mesh (Element Order – Quadratic; Free Face Meshing Type – Quad). For zone 4, the following global mesh settings were used: Element Order – Linear, Element Size – 5 mm, Capture Curvature – Yes, Curvature Min Size – 25 μm, Curvature Normal Angle – 18°.

The finite-volume mesh consists the $2.5 \cdot 10^6$ elements and has the following quality indicators: minimum orthogonal quality 0.02 (with an acceptable value greater than 0.001); maximum skewness 0.94 (with an acceptable value less than 0.95), and elements growth coefficient is equal to 57.

After building the finite-volume mesh, the next step is the surfaces set up that are necessary to set the boundary conditions and the dynamic mesh. (ensuring the possibility of the emitter disk movement). The surfaces are shown in Figure 2.

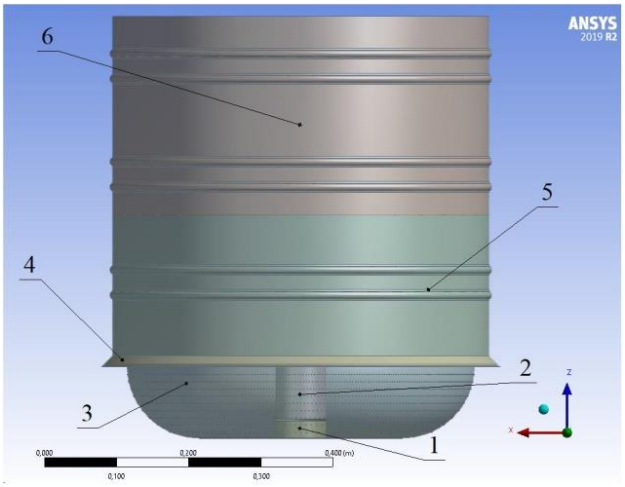

Figure 1 – Three-dimensional computational mesh

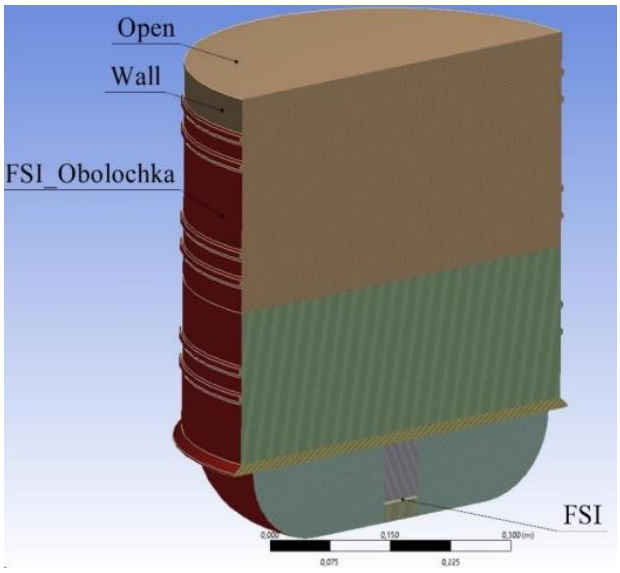

Figure 2 – Boundary conditions

The settings for the Fluent Flow module were as follows. The non-stationary analysis type was selected. Gravity force is considered with gravitational acceleration vector direction - opposite to the OZ-axis positive direction. The next is choosing a multiphase flow model – “Volume of Fluid”, which is recommended for cases

characterized by a clear distinction between the volumes of the two phases. The water was chosen as a primary phase and the air as a secondary phase. For the model was set with the following options: interface modeling type – Sharp, which is used in cases with the free liquid surface. The "Explicit" formulation uses a sequential-linear function for approximation of the interface shape between two phases.

The Implicit Body Force Formulation setting can consider the acting volumetric forces, including this will improve the problem convergence due to the partial equilibrium of the pressure gradient and volumetric forces in the momentum equation. One more critical setting is the Volume Fraction Cutoff – $1 \cdot 10^{-6}$ and Courant Number – 0.25. The conditions for the phase interacting are additionally set, namely, the surface tension forces modeling at the air/water interface with a coefficient of 0.075 N/m. The "laminar model" was chosen as a fluid flow model.

Consider the setting of boundary conditions in more detail. The "FSI", "wall", "FSI_Shell", and "open" surfaces were chosen as a wall with the "No Slip" condition, which means that the fluid velocity on all walls is equal to the wall velocity. As the operating conditions, a pressure equal to atmospheric pressure and the "operating density" as the air density was selected. This setting eliminates the hydrostatic pressure increasing in the lowest density phase, improving the rounding accuracy for impulse balance.

One of the essential steps in calculating the related problems is the dynamic mesh setting. The "Smoothing" dynamic mesh method was selected in the Fluent module. Using this method is less expensive than other methods since the node's number, and the connections between them do not change. As an additional parameter, the "Spring Contact Factor" was chosen, which makes it possible, if necessary, to ensure the position preservation of the nodes that are near the walls. After selecting the mesh rebuilding method, it is required to specify the boundaries movement type and mesh zones. The next stage is solver setup. Initially, a numerical algorithm for the pressure and velocity relationship is selected, which uses a combination of continuity and momentum equations and derivation of pressure equations. In this case, the Coupled method was chosen, although it is more computationally expensive than others, while it is more accurate. The next step is choosing the spatial discretization method, namely for pressure – "Presto!", since a pressure jump occurs at the interface; for gradient – Least-Squares Cell-Based, recommended for unstructured meshes and is the least computationally expensive in comparison with other schemes; for the momentum – Second Order Upwind, is a second-order scheme of the accuracy; for a volumetric fraction – Geo-Reconstruct, is selected automatically when the "Explicit" formulation is selected; for time – First Order Upwind. After the solver setup, initialization is required. To fill zones 1–5 with liquid, the "Patch Interface" and "Refinement Criterion" tool was used, which allows selecting the region size filled with water while accuracy the mesh in it. As additional settings, "Volumetric Smoothing" was selected, and the "Smoothing Relaxation Factor" was set to 0.25, which ensures the interface precision between phases. The last step in setting up the Fluent Flow module is the maximum number of iterations in a single time step. For ensuring the accuracy of the solution, 30 iterations were specified. After configuring the Fluent Flow module, the next step is to set up the Transient Structural module, which begins with material selection for each structural element.

In this case, the steel was selected. The linear elements were used to create the finite-element mesh were used, which are less computationally expensive and provide sufficient accuracy. Another solution feature is setting all parameters in the system SI, therefore $\omega = 2260\ s^{-1}$, and $A \cdot \omega = 0.113$ (m/s). The emitter disk's bottom and side surfaces were specified as FSI, a boundary condition that indicates that the communication between the two modules occurs through this surface. The "FSI Shell" is the surface through which the coupling calculation passes too.

The "System Coupling" module setting is the final step, in which the time step will be used for both modules is set up. It was calculated for the providing 10 substeps in one oscillation period ($T = 2.7$ ms). Therefore, the time step is equal to 0.27 ms. After that, the data transfer between the preselected surfaces in both modules is configured, namely from "FSI_Shell" (Fluent) to "FSI_Shell" (Transient Structural), the force with which the fluid acts on the surface is transferred. This means that the calculation in Fluent is the source for the Transient Structural module. For a pair of "FSI" surfaces, the Transient Structural module serves as the source of displacement for Fluent boundary.

3.2 The mathematical model

For a preliminary characteristics' assessment of the bucket vibrations, a traditional discrete mathematical model is used, which considers the inertial, stiffness, and damping functional elements properties (Figure 3) [13]:

$$m\ddot{x} + b\dot{x} + cx = F(t), \quad (1)$$

where $F(t)$ – an external force; m – the equivalent mass; c – the stiffness coefficient; b – the damping coefficient evaluated according to the numerical experiment.

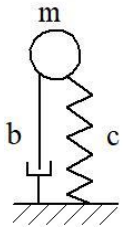

Figure 3 – The simplified model

To determine the unknown model parameters, namely the damping coefficient n, was used the data obtained in the simulation of forced vibrations bucket under the single external force action using the ANSYS software package. As noted above, the frequency of oscillation of the "effective surface area" of the perforated bucket is 231 Hz,

which corresponds to the frequency of free, undamped oscillations of 205 Hz. Therefore, the damping coefficient is determined by the formula [14]:

$$n = \sqrt{\omega_0^2 - \omega^2}, \quad (2)$$

ω_0 – frequency of free undamped oscillations.

Calculating from this formula, the damping coefficient is 107 Hz.

In the periodic external force presence, this model is reduced to a dimensionless form:

$$\ddot{x} + 2n\dot{x} + \omega_0^2 x = a_0 sin\omega t, \quad (3)$$

were a_0 – vibration acceleration amplitude of the emitter disk; n = 0,5b/m – the damping coefficient; ω_0 – self-frequency of the system.

The method of complex amplitudes [15] was used to solve the above differential equation:

$$x = Ae^{i\omega t}; \dot{x} = i\omega Ae^{i\omega t}; \ddot{x} = -\omega^2 Ae^{i\omega t}. \quad (4)$$

After substituting the equations (4) into the formula (3)

$$-\omega^2 Ae^{i\omega t} + 2ni\omega Ae^{i\omega t} + \omega_0^2 Ae^{i\omega t} = a_0 e^{i\omega t} \quad (5)$$

after identical transformations, the amplitude of the bucket oscillations was obtained:

$$A = \frac{a_0}{|\omega_0^2 - \omega^2 + 2ni\omega|} = |A|e^{i\varphi}, \quad (6)$$

where the dependence for determining the amplitude and phase of the bucket oscillations are as follows [16]:

$$\begin{cases} |A| = \dfrac{a_0}{\sqrt{(\omega_0^2 - \omega^2)^2 + (2n\omega)^2}}; \\ \varphi = arg\left(\dfrac{2n\omega}{\omega_0^2 - \omega^2}\right). \end{cases} \quad (7)$$

4 Results and Discussion

4.1 Vibration effect of the emitter disk on the priller's perforated body

The calculation results analysis begins with assessing the deformations caused by emitter disk oscillations, indicated in Figure 4. The priller body maximum deformations are placed under the disk and equal 70 μm, which means that an "effective disk area" term can be introduced, which is equal to 24 %.

To better understand the effect of the oscillations on the surface, consider the flow structure between them - the velocity vectors are shown in Figure 4 at times corresponding to the extreme lower disk position. As shown in Figure 5, flow eddies are formed on the sides during the disk movement, which means that fluid movement must be taken into account in the mathematical model creating.

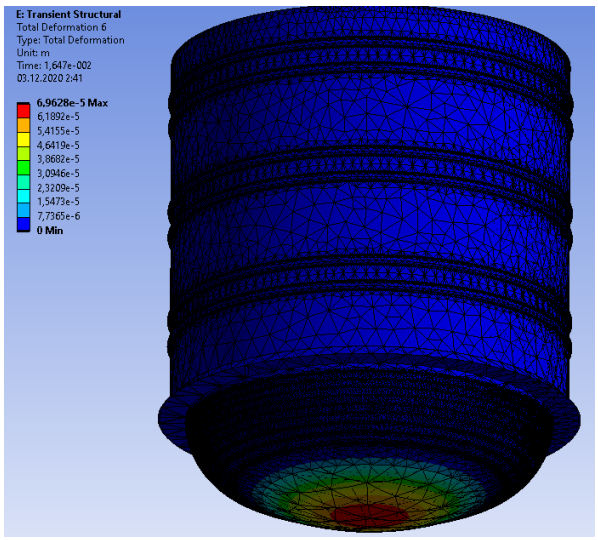

Figure 4 – The maximum deformation of the body

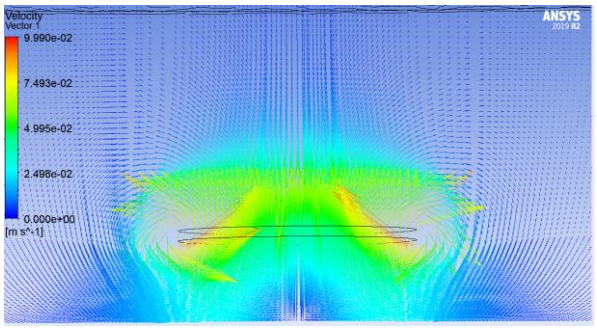

Figure 5 – Fluid velocity vectors

Let us consider in more detail the movement of the cylindrical body and the perforated bucket under the emitter disk action. Figure 6 shows the movement trajectory of the effective part of the bucket. As it can be seen, it is a cosine curve. To determine the amplitude and frequency of oscillations, we apply the fast Fourier transform, which allows us to decompose the oscillations into elementary (harmonic) components

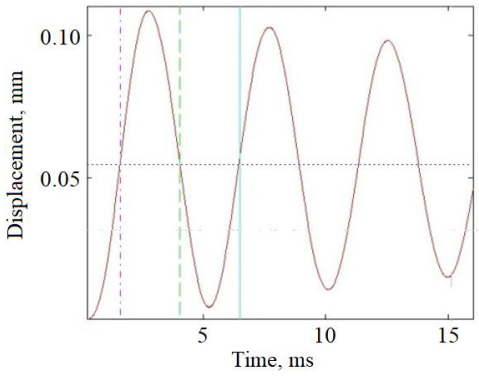

Figure 6 – The trajectory of the lower bottom point

The matrix of the perforated bucket maximum displacements, and therefore the point located under the emitter disk center, was imported into MathCAD. In this case, 64 points were used, the frequency of the points output was 3704 s^{-1}. in Figure 7, the dataset is shown.

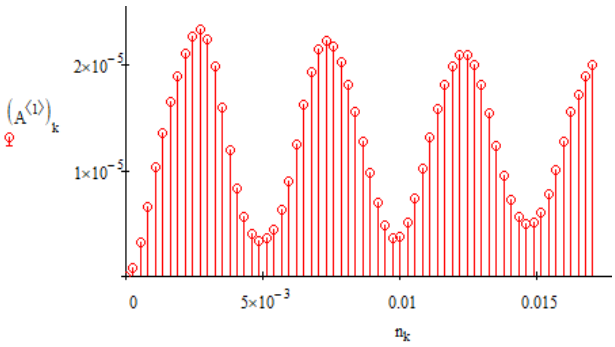

Figure 7 – The initial condition for the Fourier transform

Consider the side surfaces' vibrations perforated bucket, their deformation, and movement trajectory shown in Figures 8 a and b, respectively. Considering the obtained results, we will carry out a fast Fourier transform to obtain the harmonic components of the perforated bucket part's oscillations.

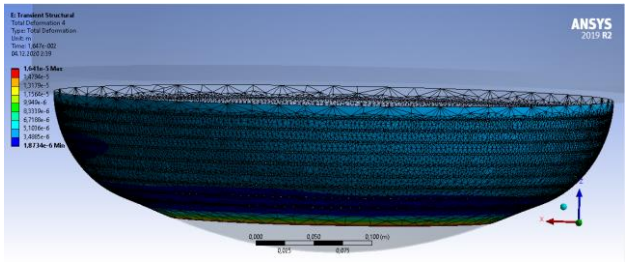

a

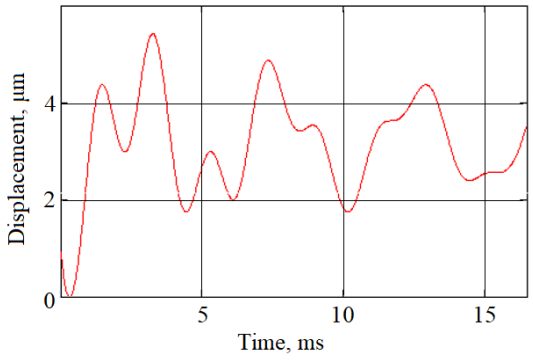

b

Figure 8 – The total deformations of the perforated bucket part (a), and the dependence of the total deformation on time (b)

As in the previous case, MathCAD is used for transformation, into which the matrix of maximum displacements of the side surfaces of the perforated bottom was imported. In this case, 64 points were used, the frequency of points output was 3704 s^{-1}. The dataset is shown in Figure 9.

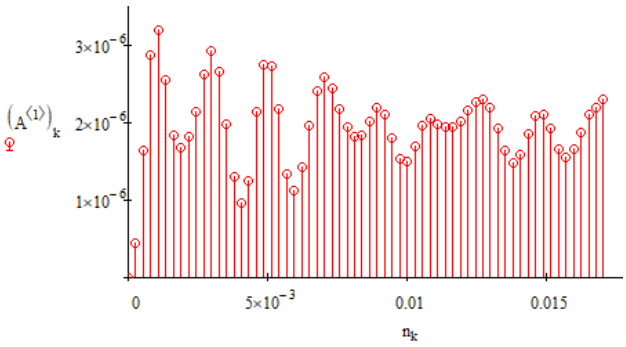

Figure 9 – The initial condition for the Fourier transform

4.2 Modal analysis

To carry out modal analysis using ANSYS Workbench in the boundary conditions computational geometry, were set using “Fixed Support” and the emitter disk was excluded from the calculation. As a result, the forms and frequencies of natural vibrations of the priller body were obtained. They are indicated in Figures 10 a and b, respectively.

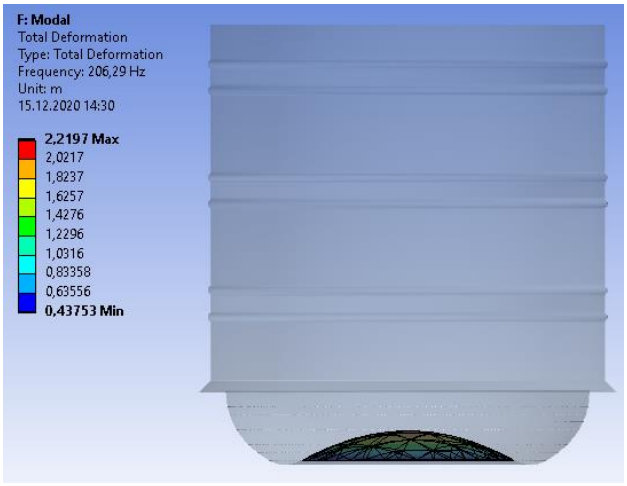

a

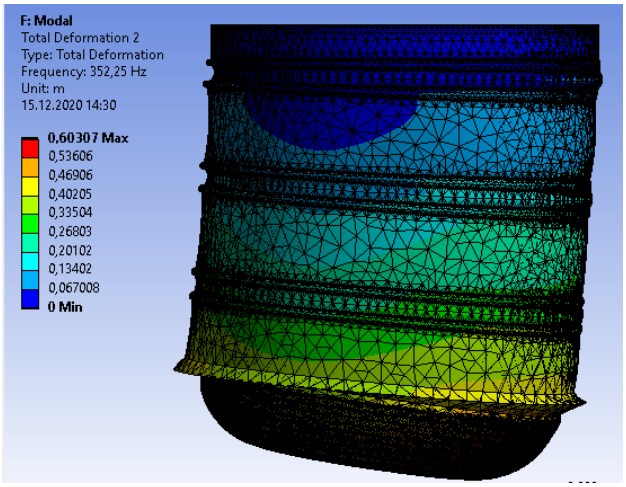

b

Figure 10 – The 1st (a) and the 2nd (b) mode shapes

The vibration nature on the second form explains the asymmetry of the middle part of the perforated bucket's deformations.

4.3 Mathematical model parameter identification

Using the linear regression procedure, parameter identification of this model of the forced oscillations can be based on the following least square error function:

$$R_1(\omega_0, n) = \sum_{k=1}^{N}[(\omega_0^2 - \omega_k^2)tg\varphi_k - 2n\omega_k]^2, \quad (8)$$

minimization of which for N experimental values (k is an experimental point number)

$$\begin{cases} \frac{\partial R_1}{\partial(\omega_0^2)} = 2\sum_{k=1}^{N}[(\omega_0^2 - \omega_k^2)tg\varphi_k - 2n\omega_k]tg\varphi_k = 0; \\ \frac{\partial R_1}{\partial n} = -4\sum_{k=1}^{N}[(\omega_0^2 - \omega_k^2)tg\varphi_k - 2n\omega_k]\omega_k = 0 \end{cases} \quad (9)$$

allows obtaining the system of linear equations:

$$\begin{cases} a_{11}\omega_0^2 - a_{12}n = b_1; \\ a_{12}\omega_0^2 - a_{12}n = b_1, \end{cases} \quad (10)$$

where the following coefficients have been introduced:

$$a_{11} = \sum_{k=1}^{N} tg^2\varphi_k\,;\; a_{12} = 2\sum_{k=1}^{N}\omega_k tg\varphi_k\,; \\ a_{22} = 2\sum_{k=1}^{N}\omega_k^2\,;\; b_1 = \sum_{k=1}^{N}\omega_k^2 tg^2\varphi_k\,; \\ b_2 = \sum_{k=1}^{N}\omega_k^3 tg\varphi_k\,. \quad (11)$$

Solving the system (10) allows evaluating the eigenfrequency ω_0 and the damping coefficient n:

$$\omega_0 = \sqrt{\frac{a_{12}b_2 + a_{22}b_1}{a_{11}a_{22} - a_{12}^2}}; n = \frac{a_{11}b_2 + a_{12}b_1}{a_{11}a_{22} - a_{12}^2}. \quad (12)$$

Remarkably, if the phases φ_k cannot be measured experimentally, the parameter identification can be based on the another least square error function:

$$R_2(\omega_0, n) = \sum_{k=1}^{N}\left[(\omega_0^2 - \omega_k^2)^2 + 4n^2\omega_k^2 - \left(\frac{a_0}{A_k}\right)^2\right]^2, \quad (13)$$

minimization of which by solving the system of nonlinear equations

$$\begin{cases} \frac{\partial R_2}{\partial(\omega_0^2)} = 4\sum_{k=1}^{N}\left[(\omega_0^2 - \omega_k^2)^2 + 4n^2\omega_k^2 - \left(\frac{a_0}{A_k}\right)^2\right](\omega_0^2 - \omega_k^2) = 0; \\ \frac{\partial R_2}{\partial(n^2)} = 8\sum_{k=1}^{N}\left[(\omega_0^2 - \omega_k^2)^2 + 4n^2\omega_k^2 - \left(\frac{a_0}{A_k}\right)^2\right]\omega_k^2 = 0 \end{cases} \quad (14)$$

after identical simplifications and not considering the trivial solution $\omega_0 = 0$ allows obtaining the following parameters:

$$\begin{cases} \omega_0(n) = \sqrt{\frac{1}{N}\left[\sqrt{a_{22}^2 + N(c_2 - c_1 - 4a_{22}n^2)} - a_{22}\right]}; \\ n(\omega_0) = \frac{1}{2}\sqrt{2\omega_0^2 + \frac{c_2 - c_1 - N\omega_0^4}{a_{22}}}, \end{cases} \quad (15)$$

where the additional coefficients are introduced:

$$c_1 = \sum_{k=1}^{N}\omega_k^4\,;\; c_2 = \sum_{k=1}^{N}\left(\frac{a_0}{A_k}\right)^2\omega_k^2. \quad (16)$$

Notably, the parameters (15) can be solved using the simple iteration procedure.

Thus, the ANSYS Workbench software with the Fluent and Transient Structural modules was used to numerically simulate the vibrational gel granulation process in an active hydrodynamic medium. Based on the numerical simulation results and their analysis using Fourier transformations, it was determined that the oscillations of the lower part of the bucket, consisting of two harmonic oscillations that equal 230 Hz and 520 Hz, which differ by almost two times. According to the modal analysis results of the priller body, it was determined that the self-vibrations first frequency is 205 Hz, and the second is 380 Hz, the third is 450 Hz, and the fourth is 550 Hz.

5 Conclusions

The paper considers the problem of numerical modeling of the gel vibration granulation process in an active hydrodynamic medium. Model development for process calculation is described. The three-dimensional computational geometry was designed, which additionally dividing into zones. These zones were used in designing a finite-volume mesh to ensure the accuracy of the calculations. The resulting mesh consists of $2.5 \cdot 10^6$ elements and has the following quality indicators: orthogonal quality 0.02 (with an acceptable value greater than 0.001); maximum skewness 0.94 (with an acceptable value less than 0.95) and elements growth coefficient is equal to 57.

This paper also presents numerical simulation results of the emitter disk vibration effect on the cylindrical body. A discrete mathematical model is presented for a preliminary assessment of the bucket vibrations characteristics, namely, constructing an amplitude-frequency characteristic. This model considers the inertial, stiffness, and damping properties of functional elements, including determining the unknown model characteristics based on the numerical modeling results, namely the damping coefficient of damped oscillations.

6 Acknowledgments

The developed methodology was realized within the research projects “Creation of new granular materials for nuclear fuel and catalysts in the active hydrodynamic environment” (State reg. No. 0120U102036) ordered by the Ministry of Education and Science of Ukraine.

Computer means for numerical simulations were realized within the internship “CFD simulation of the heat and mass transfer processes between liquid and gas phases of the mixture flow inside of the chemical equipment” at the University of West Bohemia.

Additionally, the authors appreciate the International Association for Technological Development and Innovations for the research assistance.

References

1. Afif, A. A., Wulandari, P., Syahriar, A. (2020). CFD analysis of vertical axis wind turbine using ANSYS Fluent. *Journal of Physics: Conference Series*, Vol. 1517(1), 012062, doi:10.1088/1742-6596/1517/1/012062.
2. Ricardo, G. A. N., Noriler, D., Martignoni, W. P., Meier, H. F. (2013). Eulerian-Lagrangian analysis of multiphase flow in urea prilling process with phase changing. *Chemical Engineering Transactions*, Vol. 32, pp. 2173–2178.
3. Ali, K. (2015). Design of a spray tower for the granulation of melt. *Al-Nahrain Journal for Engineering Sciences*, Vol. 18(1), pp. 111–117.
4. Jafari, H., Idris, M. H., Ourdjini, A., Farahany, S. (2013). In situ melting and solidification assessment of AZ91D granules by computer-aided thermal analysis during investment casting process. *Materials and Design*, Vol. 50, pp. 181–190, doi: 10.1016/j.matdes.2013.02.035.
5. Srinivasan, V., Salazar, A. J., Saito, K. (2011). Modeling the disintegration of modulated liquid jets using volume-of-fluid (VOF) methodology. *Applied Mathematical Modelling*, Vol. 35, pp. 3710–3730.
6. Viktorov, S. D., Frantov, A. E., Lapikov, I. N., Andreev, V. V., Starshinov, A. V. (2016). Effect of the microstructure of ammonium nitrate granules on the detonability of composite propellants based on it. *Combustion, Explosion and Shock Waves*, Vol. 52(6), pp. 727–731, doi: 10.1134/S0010508216060137.
7. Saleh, S. N., Barghi, S. (2016). Reduction of fine particle emission from a prilling tower using CFD simulation. *Chemical Engineering Research and Design*, Vol. 109, pp. 171–179.
8. Muhammad, A., Rahmanian, N., Pendyala, R. (2013). Flow analysis of melted urea in a perforated rotating bucket. *Applied Mechanics and Materials*, Vol. 372, pp. 340–345.
9. Skydanenko, M., Sklabinskyi, V., Saleh, S. (2019). CFD simulation of ammonium nitrate melt in a perforated rotating bucket. *Advances in Design, Simulation and Manufacturing. DSMIE 2018. Lecture Notes in Mechanical Engineering. Springer, Cham*, pp. 598–506, doi: 10.1007/978-3-319-93587-4_52, 498-506.
10. Li, Z., Kind, M., Gruenewald, G. (2010). Modeling fluid dynamics and growth kinetics in fluidized bed spray granulation. *The Journal of Computational Multiphase Flows*, Vol. 2(4), pp. 235–248.
11. Shimasaki, S., Taniguchi, S. (2011). Formation of uniformly-sized droplets from capillary jet by electromagnetic force. *Applied Mathematical Modelling*, Vol. 35(4), pp. 1571–1580, doi: 10.1016/j.apm.2010.09.033.
12. Saleh, S. N.; Saaed, O., Skydanenko, M. (2019). CFD assessment of jet flow behavior in an alternative design of a spray dryer chamber. *Advances in Design, Simulation and Manufacturing II. DSMIE 2019. Lecture Notes in Mechanical Engineering. Springer, Cham*, pp. 863–870, doi: 10.1007/978-3-030-22365-6_86.
13. Zhang, J., Richards, C. M. (2006). Dynamic analysis and parameter identification of a single mass elastomeric isolation system using a Maxwell-Voigt model. *Journal of Vibration and Acoustics*, Vol. 128(6), pp. 713–721, doi: 10.1115/1.2345676.
14. Chen, S., Cong, B., Zhang, D., Liu, X., Shen, S. (2020). An undamped oscillation model with two different contact angles for a spherical droplet impacting on solid surface. *Vestnik Samarskogo Gosudarstvennogo Tekhnicheskogo Universiteta, Seriya Fiziko-Matematicheskie Nauki*, Vol. 24(2), pp. 390–400, doi:10.14498/VSGTU1761.
15. Zheng, W., Cui, X., Chen, H., Zheng, R. (2020). Swept-sine integration method for complex amplitude extraction of swept-sine signal. *Journal of Mechanical Science and Technology*, Vol. 34(12), pp. 4981–4988, doi:10.1007/s12206-020-1103-6.
16. Ni, S., Chen, Q. (2011). Dynamic research on vibration-impact crushing system of a bilateral single-mass. *Advanced Materials Research*, Vol. 308–310, pp. 1914–1917, doi: 10.4028/www.scientific.net/AMR.308-310.1914.